ORGANIC SOLAR CELLS: A REVIEW

G. A. CHAMBERLAIN

Shell Research Ltd., Thornton Research Centre, P.O. Box 1, Chester CH1 3SH (Gt. Britain)

(Received March 22, 1982; accepted April 22, 1982)

Summary

The status of organic solar cell research is reviewed. The field is still in the early stages of development, but conversion efficiencies in sunlight of about 1% have been achieved. Special emphasis has been given to doping effects, carrier photogeneration and recombination. Improved understanding of the photovoltaic mechanism and the wide-ranging possibilities of molecular tailoring suggest that ultimate efficiencies of around 10% in Schottky barrier devices should be within reach.

1. Introduction

Photovoltaic solar energy conversion can be achieved by a number of different materials with different efficiencies but as yet no particular material or combination is cheap enough to compete with large-scale fossil-fuel-generated electricity. While intensive research and development are being carried out to reduce the cost of conventional inorganic devices, there is considerable interest in thin film devices which may offer an alternative investment in the longer term. In this review the progress made in one area of thin film research, namely organic solid state cells, is summarized.

Research on photovoltaic effects in organic cells began to a large extent in the 1950s when several groups [1, 2] measured the photo-e.m.f.s of various organic semiconductors on inorganic substrates. Photovoltages up to 1 V were observed. These encouraging results, coupled with the possibilities of tailoring the organic molecular structure to improve the photocurrent and of producing low cost photocells, have led researchers to look afresh at solar cells based on organic semiconductors. Remarkable progress has been made in recent years in improving the sunlight efficiency from about 10^{-5}% in the early 1970s to about 1% recently. It is generally accepted, however, that cell efficiencies must be as high as possible and at least 5% to offset area-related costs arising from encapsulation materials, support structures etc. Therefore, further improvements are necessary and the research to date has mainly focused on obtaining a greater understanding of the mechanism of operation

0379-6787/83/0000-0000/$03.00

of these devices so that their ultimate efficiency can be evaluated and perhaps achieved in practice.

2. Device structures, components and sunlight conversion efficiencies

The early work [1, 2] suggested that a photovoltaic effect will be observed if a sandwich cell consisting of a low work function metal, an organic layer and a high work function metal (or conducting glass) is illuminated. A typical cell is illustrated in Fig. 1. The organic material is almost invariably p type in its dark electrical behaviour owing to the presence of electron-trapping impurities; these in general have defied identification, although O_2 is a strong suspect [1, 3].

The devices usually behave as metal–insulator–semiconductor (MIS) structures because of the presence of a thin interfacial oxide layer which grows on the low work function metal surface. A rectifying contact is formed with the p-type organic layer and the forward diode characteristic is usually similar to that of the minority carrier tunnel diode described by Shewchun and coworkers [4, 5]. Detailed studies of the forward characteristic have revealed much information about the concentration, the energy distribution and the position of traps which exist in the forbidden gap of the organic semiconductor, as well as the influence of these traps on the carrier mobility. The presence of the oxide layer usually also results in an improve-

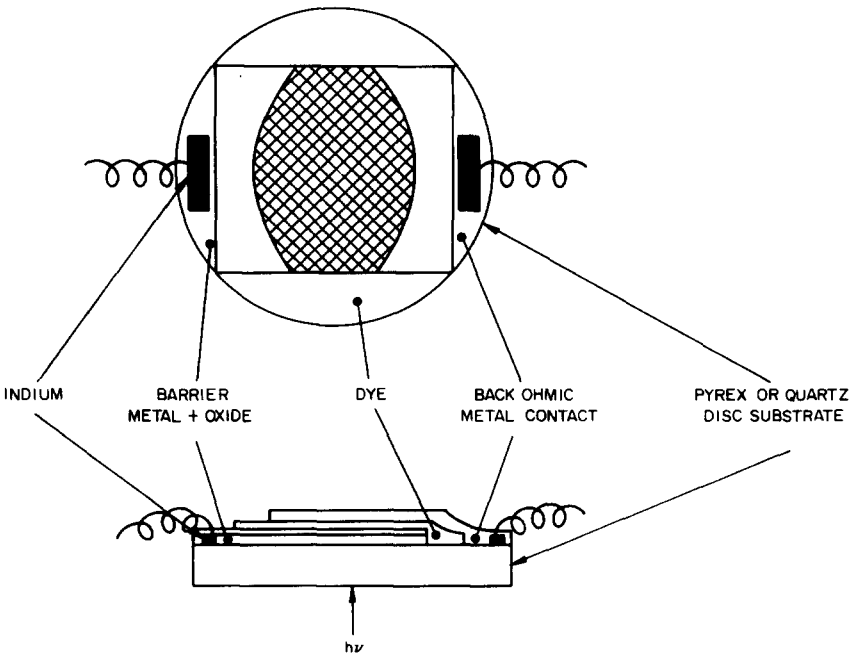

Fig. 1. A typical organic photovoltaic cell: ▩, active area.

ment in the open-circuit photovoltage, as is found in inorganic Schottky barrier diodes [6].

The low work function metal has often been aluminium and sometimes indium. Aluminium (work function, 4.2 eV) can be readily vacuum deposited onto clean substrates in thin layers so that a substantial fraction of the incident solar energy is transmitted. The conductivity of these thin layers is high enough for resistance losses to be negligible for the current densities and areas of the laboratory devices reported so far. In contrast, indium (work function, 4.1 eV) has a fourfold higher resistivity and readily forms oxides. Some difficulty has been experienced in obtaining thin transparent layers of indium without significant resistance loss. Where indium has been used as the barrier metal, the resistance loss has been overcome by evaporating an overlayer of aluminium [7] or by using very thick films with a transparency of only a few per cent. Hsiao *et al.* [8] found that a critical thickness, corresponding to a transmittance of 1%, was required to give a sheet resistivity of 5 $\Omega/\square$. In some cases a conducting glass (indium tin oxide (ITO)) substrate has been used as the back ohmic contact and illumination of the rectifying junction (or, as it is sometimes called, the depletion or barrier or space charge layer) has been achieved through this contact. However, significant light absorption by the field-free bulk of the organic layer can lead to reduced conversion efficiencies.

The inert substrate usually presents no problems and cells have been made on Pyrex, quartz, Mylar and polyester. The substrate should be thoroughly degreased and dust free. Additionally, we have observed that a rapid and reliable method of substrate (Pyrex) preparation is to preflame the bare surface in a roaring gas flame for about 10 s. This process introduces a high density of nucleation sites [9] and improves the uniformity of the aluminium thin film, which in turn leads to reproducible electrical and optical behaviour.

The back contact should be electrically non-blocking (ohmic), and gold, silver and conducting (ITO) glass have proved to be suitable because of their high work functions.

The organic material should be chosen or tailored to meet a number of requirements and it is not difficult to understand why porphyrinic-type molecular films have received intensive study.

(a) The compounds are easy to prepare and purify, and they have long shelf lives.

(b) They are highly coloured; in particular, the phthalocyanines have absorption coefficients greater than 10^5 cm^{-1} in the visible region over relatively large wavelength ranges.

(c) Thin polycrystalline films are readily formed by vacuum sublimation and are stable in air. The planar nature of the molecular ring appears to confer a degree of self-orientation to the solid state structure.

(d) The semiconductor properties of these molecular solids are well documented. For example, Fan and Faulkner [7] measured a rectification ratio of 10^3 at 0.8 V for an indium–zinc phthalocyanine (ZnPc) rectifier.

TABLE 1

Progress in organic solar cells

Date	*Cell*	η_s [a] (%)	ϕ_ϵ [b] (%)	V_{oc} (V)	*FF*	*Stability*	*Reference*
1973	Al/tetracene/Au	$<10^{-4}$	—	0.65	0.55	Not tested	[12]
1974	Al/MgPc/Ag	$<10^{-3}$	0.15	0.85	0.25	Not tested	[13]
1975	Cr/chlorophyll-a/Hg	$<10^{-3}$	0.7	0.32	0.25	Slow decay in air and light	[14, 15]
1977	Ga/squarylium dye/In_2O_3, Br_2 doped	0.05	2.3	0.65	0.37	Slow decay	[16, 17]
1977	Pt/crystal violet/tin oxide	0.002	—	0.34	—	Poor	[18]
1977 - 1978	Tin oxide/CuPc/pyrylium dyes/In	0.5	—	0.43	0.44	Not tested	[10]
1977	Al/OEP/Ag	<0.01	3.4	0.6	—	Not tested	[19]
	Al/TPP/Ag		0.9	0.6	—	Not tested	
1978	Al/H_2Pc/Au	$<10^{-3}$	0.14	0.8	0.3	Decay to steady value	[20]
	Al/ZnPc/Au	$<10^{-3}$	0.06	—	—	Decay to steady value	
1978	In/H_2Pc/Au	—	3.9	0.25	0.25	Good	[20]
	In/ZnPc/Au	<0.01	14.2	0.22	0.48		
1978	Al/merocyanine 5/Ag	0.7	33	1.2	0.25	Good in inert atmosphere	[21, 22]
1978	Al/InPcCl/SnO_2	0.3	4.5	0.67	0.4	Not tested	[23]
1979	Al/H_2Pc in polymer/tin oxide	≈ 0.01	62	1.1	0.33	Unstable, output dropped as light intensity increased	[24]
1979	In/H_2Pc in PVK/NESA	≈ 0.01	35	0.4	0.33	Good	[8]
1979	NESA/CuPc/perylene derivative/Ag	1.0	—	0.44	0.6	Not tested	[11]
1979	Hg/chlorophyll/surfactant plastoquinone/Al	<0.01	0.2	0.27	—	Not tested	[25]
1979	Sm/PVK:TNF/tin oxide	1.6×10^{-4}	—	0.82	—	Not tested	[26]
1979	TiO_2/merocyanine 5, I_2 doped/Au	—	12	—	0.44	Good in vacuum	[27]
1980	Al/Mg TPP/Ag	—	10	—	—	Not tested	[28]
1981	Al/$(CH)_x$/electrodag	0.006	10 - 100	0.31	0.21	$(CH)_x$ oxygen sensitive	[29]
1981	Al/$(CH)_x$, HCl doped/Au	0.01	—	0.4	0.25		[30]

TABLE 1 *(continued)*

1981	In/H_2Pc in polymer/NESA	0.02	73	0.45	0.33	Stable output indicated	[31]
1981	Al/merocyanine/ITO	0.2	—	≈ 1.1	≈ 0.25	Slow decay in air	[32]
	Ag/merocyanine/ZnO/ITO/polyester	0.1	—	≈ 0.45	0.3	Reasonably good in air	

[a] Sunlight efficiency based on incident photons.
[b] Quantum yield at peak absorption based on light absorbed. H_2Pc, hydrogen phthalocyanine; MgPc, magnesium phthalocyanine; NESA, conducting glass substrate; OEP, octaethyl porphyrin; PVK, poly(vinyl carbazole); TNF, trinitrofluorenone; TPP, tetraphenylporphyrin.

(e) The conductivity can be altered by suitable doping.

(f) The ground and excited states readily undergo redox reactions with suitable reagents, not only via the π system of the organic ring, but also by a change in the oxidation state of the metal complexed at the centre.

(g) The natural photosynthetic system is based on chlorophyll, a magnesium porphyrin.

Despite these properties, however, continuous evaporated thin films of the porphyrins and phthalocyanines do not exhibit high solar conversion efficiencies even when they are doped. The merocyanine class of dyes appears to have better carrier generation and collection efficiencies, and solar efficiencies of up to about 1% have been reported in recent years.

A notable exception to these MIS–Schottky barrier cells is a highly efficient device made by workers at Kodak laboratories [10, 11]. In a series of patents, they claim that a photoactive layer exists at the junction between copper phthalocyanine (CuPc) and various other photoconductors. The devices appear to be similar in operation to p–n heterojunction cells in which the p layer is CuPc and the n layer is a pyrylium dye or perylene derivative. Ohmic contacts are provided by ITO glass and indium respectively.

A survey of the progress made in organic solar cells is given in roughly chronological order in Tables 1 and 2. The chemical formulae of the compounds used are shown in Fig. 2. The rate of improvement in sunlight conversion efficiency, roughly an order of magnitude per year, has been brought about by an increased understanding of the mechanisms of junction

TABLE 2

Progress in organic solar cells[a]

Date	*Cell*	η_s (%)	ϕ_e (%)	V_{oc} (V)	*FF*	*Stability*
1977	Al/MgPc/Au O_2, H_2O doped	$\approx 10^{-3}$	0.5	1.0	0.25	Good in vacuum
1978	Al/CuPc/Au O_2, H_2O doped	$\approx 10^{-3}$	0.5	0.8	0.34	Good in vacuum
1978	Al/CuPc/Au I_2 doped	0.01	3	0.6	0.34	Good in vacuum, slow decay in air
1979	Al/merocyanine 5/Ag air doped	0.01	1.2	0.85	0.28	Slow decay
1979	Al/merocyanine 9/Au I_2 doped	0.18	10	0.7	0.39	Good in vacuum
1980	Al/merocyanine 9/Au I_2 doped	0.31	12	0.7	0.35	Good in vacuum
1981	Al/merocyanine 9/Au Cl_2 doped	0.36	13.5	0.74	0.39	Good in vacuum

[a] Work carried out by Shell Research Ltd.
Source: refs. 33, 34, 35, 36.

1 CRYSTAL VIOLET

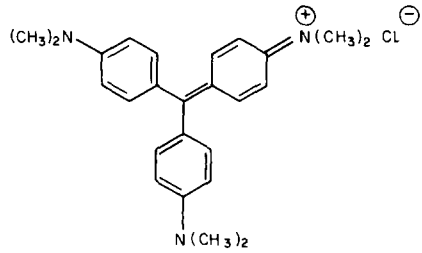

2 TETRACENE

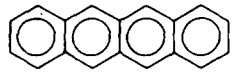

3 HYDROXYSQUARYLIUM

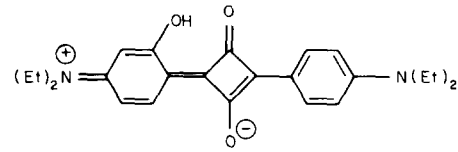

4 CHLOROPHYLL - a

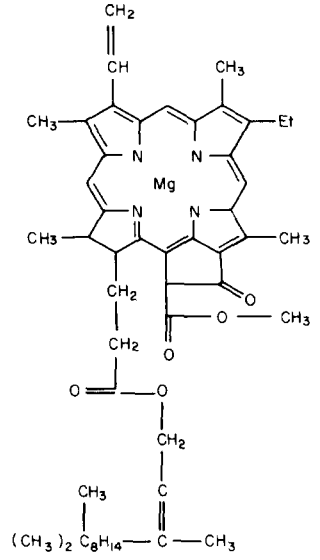

5 A MEROCYANINE: 3-CARBOXYMETHYL — 5 — [(3-ETHYL-2-(3H)-BENZOTHIAZOLIDENE) ETHYLIDENE] — 2 — THIONOTHIAZOLIDINE — 4 — ONE

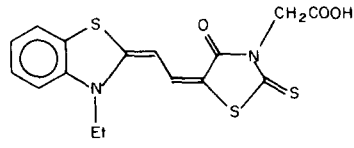

Fig. 2 *(continued)*.

6 PHTHALOCYANINE

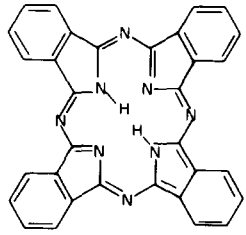

7a OCTAETHYLPORPHYRIN

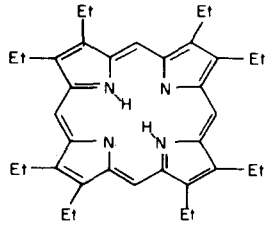

7b TETRAPHENYLPORPHYRIN

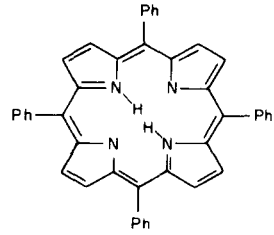

8 A PYRYLIUM DYE : 4– [(2,6–DIPHENYL– (4H)–PYRAN–4–YLIDENE) METHYL] – 2,6–DIPHENYLPYRYLIUM PERCHLORATE

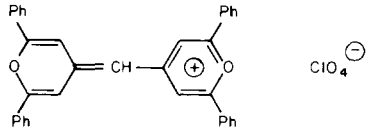

9 A MEROCYANINE : 3–ETHYL–5– [(1–ETHYL–4– (1H) –QUINOLYLIDENE) –ETHYLIDENE] –2–THIONOTHIAZOLIDINE – 4 – ONE

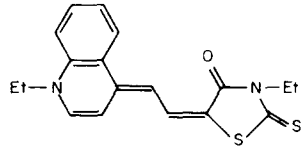

10 A MEROCYANINE : 3–ETHYL–5– (1–ETHYL–4– (1H) –QUINOLYLIDENE) – RHODANINE

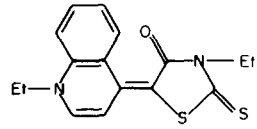

11 POLY (N–VINYL CARBAZOLE)

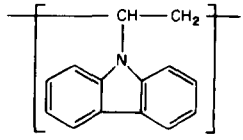

Fig. 2. Structure of organic materials used in the organic photovoltaic cells of Tables 1 and 2 and referred to in the text.

formation, oxide effects, carrier photogeneration and the dependence of photoactivity on molecular structure and device composition. However, many questions remain unanswered. In particular, the low quantum yield is still the limiting factor. In contrast, photovoltages approaching their theoretical values have been observed. Therefore, the remainder of this paper is concerned with the current state of knowledge about organic cells and with indications of some aspects that deserve greater attention.

3. Doping effects

The effects of molecular doping on the photoelectrical and dark electrical behaviour of organic materials are well known, if not entirely understood. It is surprising, therefore, that many studies of the photovoltaic response in the literature have neglected the influence of atmospheric exposure, in particular exposure to oxygen and water vapour. By making a complete cell *in vacuo*, we have found [33, 34] that an exposure to ambient air of only a few seconds is required to obtain a photoresponse and that, before doping, the photoresponse is very small and in some cases barely detectable. This behaviour is applicable to all the p-type organic materials that we have studied, *i.e.* porphyrins [37], phthalocyanines, merocyanines and cyanines. Dopants with greater electronegativity than oxygen, such as halogens, NO_2 etc., result in an even greater enhancement of the photovoltaic response.

3.1. Photoconductivity cells

There have been many studies, however, of the effect of dopants on the dark conductivity and photoconductivity of surface and sandwich conductivity cells. The early results have been collected by Meier [3]. The main conclusions are as follows.

(a) Dopants with high electron affinity (*e.g.* chloranil, iodine, tetracyanoquinodimethane (TCNQ) and tetracyanoethylene) act as acceptors, and dopants with low ionization energies (*e.g.* alkali metals) act as donors. These acceptors and donors can increase the carrier concentration and hence the dark conductivity, as in inorganic semiconductors.

(b) The addition of dopants reduces the thermal activation energy of the dark conductivity.

(c) There are marked concentration effects. The dark conductivity increases with the concentration of dopant up to a maximum value at high doping levels; this is followed by a decrease in the dark conductivity where the conductivity is dominated by direct coupling between dopant molecules [38].

(d) At low concentrations of acceptor dopants the photoconductivity of p-type organics can change by several orders of magnitude, whereas the dark conductivity increases only slightly.

(e) The generation of neutral mobile excited states (excitons) is of central importance in the formation of charge carriers and in the transport of excitation energy in the organic material.

In recent years, Wright and coworkers [39] have observed the magnitude, rate and reversibility of changes in the surface semiconductivity of single crystals of phthalocyanines, perylene, TCNQ and molecular complexes as a function of the ambient gas. $NO_2 + N_2O_4$ increases the surface conductivity of phthalocyanines by factors of up to 10^8. The reversibility of this effect by heating *in vacuo* depended on the metal complexed in the phthalocyanine, *i.e.* metal-free phthalocyanine, nickel phthalocyanine (NiPc), CuPc and ZnPc are more reversible than cobalt phthalocyanine and manganese phthalocyanine which in turn are more reversible than lead phthalocyanine. Treatment with low pressures of NH_3 gave a rapid reversal of the effect. The surface conductivity of perylene was enhanced by a factor of 10^8 in BF_3. These conductivity changes are interpreted in terms of the production of ionized states after weak chemisorption involving donor–acceptor interactions. The maximum conductivity enhancement was consistent with complete surface coverage by adsorbed molecules, each surface site producing one ionized state.

The surface photoconduction [40], however, was more sensitive than the semiconduction to low concentrations of NO_2 and BF_3. Photoconduction in phthalocyanines was enhanced, while that in perylene was inhibited. The effects were much more difficult to reverse than the effects of the same gases on semiconductivity. The action spectra are consistent with the conclusions of Popovic and Sharp [41] that carrier photogeneration is a bulk phenomenon. Popovic and Sharp prepared sandwich cells of metal-free β-phthalocyanine and in a pulsed photoconductivity experiment showed that quantum efficiencies became larger as the light penetration depth was increased by varying the excitation wavelength. The quantum efficiency also increased from 0.025% to 0.1% over a period from 5 to 12 weeks in air, indicating that carriers were probably generated by exciton dissociation on oxygen impurity centres. In contrast, in single crystals of metal-free β-phthalocyanine, a quantum efficiency of only 10^{-6}% at 400 °C *in vacuo* was measured [42]. Under these conditions it is probable that the bulk oxygen content is very low.

In metal-free phthalocyanine, it may not only be oxygen which is responsible for increasing the carrier photogeneration. Menzel and Loutfy [43] have shown that bulk doping of the X-polymorph of metal-free phthalocyanine with metal phthalocyanines, which may be present as impurities in the starting material, can increase the carrier photogeneration and decrease the cell resistance. The photogeneration of carriers appears to be extrinsic, involving field-assisted exciplex (excited molecular complex) dissociation. This interpretation followed from an observed quadratic field dependence of fluorescence quenching.

Some insight into the mechanism of dopant adsorption and carrier photogeneration has arisen from the surface photovoltage studies of Dahlberg and Musser [44]. The dependence of the surface photovoltage of NiPc and CuPc films on the oxygen ambient was accounted for with a theoretical model involving the transfer of charge from the phthalocyanine ring to

adsorbed oxygen, resulting in the formation of $Pc^{\delta+}-O_2^{\delta-}$ charge transfer complexes. A bonding model has been proposed from symmetry arguments in which the lowest unoccupied molecular orbital π^* O_2 orbital has the correct e_g symmetry to accept electronic charge from either the two e_g orbitals (d_{xz}, d_{yz}) on the central metal ligand or the $6e_g$ orbital (the first excited state orbital) of the phthalocyanine ring. The importance of the metallic e_g orbitals in the adsorption process is not fully understood, however, since an oxygen ambient affects the electrical characteristics of metal-free phthalocyanine [45], but this compound is not catalytically active in oxidation reactions [46]. Other experiments [47] have revealed that the surface monolayer is irreversibly bound to the NiPc, whereas subsequent layers are reversibly adsorbed and can be removed by evacuation of the sample. Similar effects were observed in the surface photovoltage of metal-free phthalocyanine films with adsorbed *o*-chloranil [48].

The effect on the dark conductivity of the incorporation of iodine into thin films of NiPc has been studied by several workers. Orr and Dahlberg [49] have found that permanently conductive ($2\ \Omega^{-1}\ cm^{-1}$) films can be prepared by heating sublimed films in an iodine ambient at 140 - 200 °C. An additional absorption peak appears at 978 nm, indicating a possible charge transfer transition, and the conductivity increase has been attributed to the partial oxidation of NiPc and to the presence of chains of polyiodide counter-ions. Similarly, the highly conducting behaviour of iodine-doped polyacetylene is thought to arise from the presence of iodine as I_3^- and possibly I_5^-. One-dimensional metallic-type conductivity in this material was consistent with the observation of a finite density of states at the Fermi level in a *cis*-rich polymer film [50]. In the model compound β-carotene, iodine doping also resulted in a dark conductivity increase, and I_3^- and I_5^- were detected [51].

Evidence for the enhancement of photoconductivity by iodine in thin films of poly(vinyl chloride) (PVC) has come from the study by Bahri *et al.* [52]. They suggest that the photosensitization may be interpreted in terms of a charge transfer transition of the following form:

$$DA \overset{h\nu}{\rightleftharpoons} D^+A^-$$

where PVC is a weak donor D and iodine is the acceptor A. The results were consistent with the observation of Hoegl [53] on the systematic doping of polymers (see also ref. 3). In contrast [54], the dark bulk conductivity of disordered polymers containing acceptor dopants, which form charge transfer complexes, increases only slightly.

3.2. Photovoltaic cells

The influence of ambient air on the performance of phthalocyanine photovoltaic cells has been studied by Fan and Faulkner [20]. A freshly prepared Al/metal-free phthalocyanine/Au or Al/ZnPc/Au cell, after brief exposure to ambient air followed by storing and testing *in vacuo*, showed an

initial transient photocurrent spike at the moment of illumination; this was followed by a fall in photocurrent over a period of a few minutes to a steady level. Over a period of 1 day to several days, the short-circuit photocurrent dropped to almost one-half to one-third of the initial steady value. When the cell was removed from the vacuum and stored in dry air, the photocurrent first increased and then dropped again to a steady level which was one-third to one-half of that reached *in vacuo*. The results appear to be consistent with the idea that oxygen plays a dual role. First, oxygen is doping the phthalocyanine film and improving the carrier photogeneration efficiency. Second, an insulating layer of Al_2O_3 gradually builds up at the aluminium–phthalocyanine interface in the presence of excess oxygen (dry air) and degrades the cell performance by providing a barrier to the electron flow. We have observed [33] similar effects in Al/CuPc/Au cells. In addition, we observed a dark "battery" effect when the cell was exposed to excess air, consistent with high surface coverage of the exposed portion of the sandwich cell by oxygen and water vapour. Oxidation of the aluminium electrode occurs and the electrons released in this reaction generate a dark current. The effect disappears on re-evacuation as these weakly adsorbed surface layers are readily removed. Also, if iodine vapour is used to dope the cell without releasing the vacuum, *i.e.* if the cell is fabricated, doped and tested without ever being exposed to air, then the short-circuit photocurrent increases by several orders of magnitude and the cell does not degrade over a period of several days (the maximum test time).

Iodine doping has also been used to improve the conversion efficiency of merocyanine solar cells. Some typical results from our laboratory are given in Table 3. The dramatic effects of doping with oxygen, water and especially iodine are apparent. We have also observed that doping with Cl_2 or NO_2 instead of iodine results in a further slight increase in the quantum efficiency. Skotheim [27] has observed a fivefold increase in the mono-

TABLE 3

The Al/merocyanine/Au cell

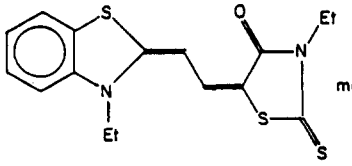

merocyanine 5

Treatment	V_{oc} (V)	I_{sc} (μA cm^{-2})	*FF*	η (%)
(1) Before doping	<0.001	0.01	—	$<10^{-8}$
(2) 0.5 atm O_2 for 10 min	0.13	0.94	0.25	0.0027
(3) H_2O vapour	0.85	7	0.28	0.015
(4) New cell, I_2 doped	0.44	31	0.35	0.042

Incident light intensity, 11.4 mW cm^{-2}; AM 2.

chromatic quantum efficiency in n-TiO_2/merocyanine/Au cells when the merocyanine layer is treated with iodine. The increase in the photoconductivity of the iodine-doped cell also led to improvements in the fill factor to 0.44.

Merritt and Hovel [16, 17] doped hydroxysquarylium cells with bromine or 1-phenyl-3-*p*-*N*,*N*-diethylaminostyryl-5-*p*-*N*,*N*-diethylaminophenyl-Δ^2-pyrazoline. Fivefold improvements in the monochromatic conversion efficiency were measured for both dopants.

Further studies are required to optimize the dopant type, concentration and distribution, but it is clear from the above results that the doping of p-type organic semiconductors with electron-accepting impurities is crucial to the generation of significant photovoltaic effects. An assessment of the data reveals that the effectiveness of dopants, applicable to merocyanines, phthalocyanines, porphyrins and possibly other p-type organic semiconductors, is given roughly by the following order: Cl_2, NO_2 (greatest effect); I_2, Br_2; organic electron acceptors (*e.g.* chloranil and trinitrofluorenone); H_2O; O_2 (much greater effect than N_2 and argon); N_2, argon (no effect). An understanding of the carrier photogeneration mechanism and of the role played by the dopant is still in its early stages, as will be revealed in Section 4.

4. Charge carrier photogeneration

The mechanism of charge carrier photogeneration in organic materials has been the subject of many studies. There exist a variety of photophysical processes, involving single-photon or double-photon excitation, which can lead to the generation of charge carriers in organic materials [1, 3, 55]. These are summarized below and, where possible, the rate probability data for crystalline anthracene (the most thoroughly investigated organic crystal) are included.

4.1. Single-photon processes

4.1.1. Direct band-to-band excitation of electrons

For anthracene, the quantum yield of this process is about 10^{-4} for photons of energy 3.9 - 5 eV, the second electronic transition.

4.1.2. Thermal excitation of excitons to give conduction band electrons and valence band holes

This process has not been observed in anthracene, probably because of the large energy differences (about 0.8 eV) between the vibrationally relaxed first exciton level and the bottom of the conduction band.

4.1.3. Exciton dissociation by direct electron transfer to the barrier metal

Baessler and coworkers [56 - 61] have studied the quenching of excitons at metal surfaces by inserting fatty acid insulating layers between the

metal and the organic material, thereby artificially increasing the reaction distance. They concluded that an exciton could undergo several reactions with the metal contact.

(i) Charge transfer with the rate constant k_{CT} which, depending on the energetics of the barrier, can be either oxidative, *i.e.*

$$M^*(S_1 \text{ or } T_1) + \text{metal} \rightarrow M^+ + (\text{metal})^-$$

or reductive, *i.e.*

$$M^*(S_1 \text{ or } T_1) + \text{metal} \rightarrow M^- + (\text{metal})^+$$

In these reactions, M^* is the exciton in a singlet or triplet state. A functional dependence of k_{CT} on distance was obtained empirically and theoretically:

$$k_{CT} = k_{CT,0} \exp\left(-\frac{x}{x_0}\right) \tag{1}$$

where x is the insulating film thickness, x_0 is the critical film thickness and $k_{CT,0}$ is equal to k_{CT} when $x = 0$.

(ii) The exciton can transfer energy to the metal electrons by resonance interaction (dipole–dipole coupling), with rate constant k_{dd}. This process is thought to be a more significant decay process for singlet excitons than for triplet excitons because of the dependence of k_{dd} on the third power of the oscillator strength of the emitting dipole. k_{dd} was found to vary with x as

$$k_{dd} = k_{dd,0} x^{-3} \tag{2}$$

(iii) The exciton can be quenched by an exchange interaction, with rate constant k_E. This process is similar to exciton dissociation by charge transfer (process (i)) and it is reasonable to expect that both k_E and k_{CT} show similar functional dependences on x. However, the exchange interaction is a three-particle process and is much less effective than charge transfer.

(iv) The exciton can be quenched by radiationless transitions induced by a paramagnetic metal electrode (rate constant k_{isc}).

Thus the efficiency of charge transfer ϕ_{CT} at a metal contact in the absence of other carrier photogeneration mechanisms is given by

$$\phi_{CT} = \frac{k_{CT}}{k_{CT} + k_{dd} + k_E + k_{isc}} \tag{3}$$

4.1.4. Exciton dissociation at impurity (dopant) sites on the surface or in the bulk

In addition to the quenching of excitons at metal surfaces, the dissociation of excitons at impurity (dopant) sites both on the surface and in the bulk of the material has been studied.

4.1.5. Optical detrapping of space charges

Funfschilling and Williams [62] and Arden *et al.* [63] have investigated the optical detrapping of space charges.

4.1.6. Photoelectric emission from the metal contact

Another photophysical process which involves single-photon excitation is photoelectric emission from the metal contact.

4.2. Double-photon processes

4.2.1. Exciton–exciton interactions

The collision of two excitons (singlet plus singlet or singlet plus triplet) can result in charge formation if the total energy is greater than that of the band gap of the semiconductor. For anthracene, the rate constants for these processes are as follows:

$S_1 + S_1 \rightarrow S_0 + h^+ + e^-$	5×10^{-12} cm^3 s^{-1}	[64, 65]
$S_1 + T_1 \rightarrow S_0 + h^+ + e^-$	10^{-12} cm^3 s^{-1}	[66]

4.2.2. Photoionization of excitons

The absorption of a second photon by a singlet or triplet exciton can result in carrier formation. For anthracene, the interaction cross sections σ are as follows:

$S_1 + h\nu$	$\sigma = 10^{-19}$ cm^2	[67, 68]
$T_1 + h\nu$	$\sigma = 10^{-20}$ cm^2	[69]

4.2.3. Double-quantum excitation

The interaction cross section for this process in anthracene is 10^{-31} cm s^{-1} [70].

All these processes should result in photocurrents that are quadratic in light intensity. In unconcentrated sunlight (about 5×10^{17} photons cm^{-2} s^{-1}), organic cells usually display sublinear light intensity dependences and linear dependences at low light intensities. In contrast, the "best" merocyanine cells have linear dependences up to sunlight intensities. Therefore, it seems probable that two-photon processes are not responsible for the charge carrier production in organic cells. These empirical results are also consistent with the predictions made on the basis of the low values of rate constants and interaction cross sections.

If we take into account the single-photon processes, and in view of the doping results, carrier photogeneration appears to be readily explained in terms of exciton dissociation at dopant sites (Section 4.1.4). Photoelectric emission from the metal contact can be ruled out, since in most cases photovoltaic action spectra follow closely the absorption spectra of the organic materials and not the metal electrodes. Optical detrapping of space charge can also be excluded because efficient cells (*e.g.* merocyanine-based cells) can sustain photocurrents equivalent to many times the upper limit of the expected trapped charge concentrations without decay. Alternatively, however, if the function of the dopant is to improve the dark conductivity, then the remaining single-photon processes may still play an important role. Explicitly, there are four possible mechanisms involving dopant species.

(1) The dopant forms acceptor surface states at the barrier metal oxide–organic interface; these aid carrier formation by accepting electrons from the exciton, *i.e.*

$$M^*(S_1 \text{ or } T_1) + (\text{surface state}) \rightarrow M^+ + (\text{surface state})^-$$

(2) The dopant increases the p-type conductivity and thereby improves the rectification properties of the barrier metal–organic junction. This is equivalent to increasing the built-in field at the interface by reducing the barrier width, *i.e.*

$$M + \text{dopant} \overset{kT}{\rightleftharpoons} M^+ + (\text{dopant})^-$$

(3) The dopant forms charge transfer complexes with the organic molecules in the thin film and excited complexes dissociate in the built-in field, *i.e.*

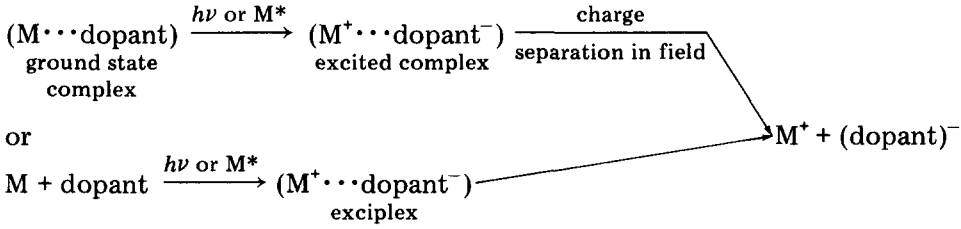

As shown above, excitation of the complex can be achieved by direct absorption of photons or by energy transfer from uncomplexed excitons.

(4) The dopant forms charge transfer complexes with the organic molecules, which then accept electrons from migrating uncomplexed dye excitons, *i.e.*

$$M^* + (M\cdots\text{dopant}) \xrightarrow{e^- \text{ transfer}} M^+ + (M\cdots\text{dopant})^-$$

As in process (3) the charge generation step must be followed by charge separation in the field. Electrons and holes are assumed to hop from one site to the next.

In order to differentiate between the four dopant mechanisms, we and others have carried out experiments on surface effects, conductivity, and field dependence of fluorescence quenching and photocurrent enhancement. In our experiments, the carrier generation at dopant-induced surface states was tested by exposing a thin (about 3 nm) aluminium oxide layer on about 10 nm aluminium to iodine vapour before evaporating the organic (merocyanine) layer. After an ohmic gold contact had been evaporated onto the back face of the merocyanine layer, a small photoresponse was observed, but the power output increased over 60-fold on exposure of the whole cell to iodine vapour. The result strongly suggests that iodine-activated surface states are not important in the generation of photovoltaic behaviour. The initial small response was probably caused by back diffusion of iodine from the oxide into the dye layer at the interface. Mechanism (2) was tested by preparing cells of the type Au/organic/Au or Al/organic/Al, where the

organic layer is merocyanine, CuPc, or magnesium or zinc porphyrin. When the organic layer was doped with iodine, using the same doping technique as for photovoltaic cells, the dark conductivity was left unchanged. This important result rules out mechanism (2).

Mechanisms (3) and (4) have been probed by noting that electric-field-assisted exciplex dissociation (mechanism (3)) predicts, on the basis of the Stark effect [71], a quadratic field dependence at all field strengths, but that mechanism (4) predicts a linear field dependence at low field strengths, on the basis of the theory of geminate recombination [72]. Preliminary conclusions on the basis of an observed linear field dependence of the photocurrent at low field strengths indicate that mechanism (4) is the dominant process in merocyanine cells [35]. Menzel and Popovic [73] observed that the fluorescence quenching of metal-free X-phthalocyanine in poly(vinyl acetate) is directly proportional to the applied field up to 1.1×10^5 V cm^{-1}. Thus, photogeneration occurs from the excited singlet state and the results can be interpreted in terms of mechanism (4). At higher fields [74], a quadratic dependence fitted the results and the present authors suspect that exciplex formation is followed by field-assisted exciplex dissociation into mobile carriers. It is interesting also that Yokoyama *et al.* [75 - 77] have observed an almost quadratic field dependence of exciplex fluorescence quenching in poly(*N*-vinyl carbazole) films doped with low concentrations of dimethylterephthalate at field strengths above 5×10^4 V cm^{-1}. All the results however can be explained in terms of mechanism (4), rather than mechanism (3). Exciplex (or excited complex) fluorescence quenching appears to be caused by field-assisted thermal dissociation of the charge transfer state into free carriers, *i.e.*

$$D^* + A \xrightarrow{e^- \text{ transfer}} (D^+ \cdots A^-)^* \begin{cases} \xrightarrow{} D^+ + A^- \\ \xrightarrow[\text{field} = 0]{} D + h\nu_f + A \end{cases}$$

The applied field, therefore, decreases the yield of geminate recombination. The acceptor A may be regarded as a charge transfer complex or an unbound acceptor molecule. The mechanism is discussed in Section 5.

In general, electric-field-induced fluorescence quenching is proving to be a useful technique for probing the mechanism of carrier photogeneration in organic materials. An important feature of this technique is that the quenching is not expected to be affected by charge trapping after carrier separation, which makes the interpretation of photocurrent measurements difficult. Additionally, the fluorescence quenching efficiency equals the quantum yield of carrier generation for small zero-field generation efficiencies.

5. Carrier recombination

A number of different models have been used to explain carrier recombination in low mobility materials. The most frequently investigated model has been the Onsager theory of geminate recombination [72]. In this theory

it is assumed that electron–hole pairs separate to an initial distance r_0 in the primary photogeneration step. In selenium [78], r_0 is strongly wavelength dependent since it is identified with the thermalization distance of a hot electron–hole pair generated by light absorption. The photoexcited carrier pair shows an excess of kinetic energy, given by $h\nu - \lambda_g + E_c(r)$ where $h\nu$ is the photon energy, λ_g is the band gap (the threshold absorption energy), r is the pair separation and $E_c(r) = e^2/4\pi\epsilon\epsilon_0 r$ is the Coulomb energy of the pair. Thus the photogeneration efficiency will not approach unity unless the carriers diffuse apart a distance greater than r_c before they thermalize, where r_c is the distance at which $E_c \approx kT$. Otherwise, geminate recombination is more probable than the creation of a free carrier pair. Using the assumption that the initial distribution of thermalized pairs is an isotropic δ function, the generation efficiency is given by

$$\phi_{ons}(r_0, F, T) = \phi_0\phi_{esc}$$

$$= \phi_0 \frac{kT}{eFr_0} \exp(-A) \exp\left(-\frac{eFr_0}{kT}\right) \times$$

$$\times \sum_{m=0}^{\infty} \frac{A^m}{m!} \sum_{n=0}^{\infty} \sum_{l=m+n+1}^{\infty} \left(\frac{eFr_0}{kT}\right)^l \frac{1}{l!} \tag{4}$$

where ϕ_0 is the efficiency of the production of thermalized pairs per absorbed photon, ϕ_{esc} is the escape efficiency, $A = e^2/4\pi\epsilon\epsilon_0 kTr_0$ and F is the field strength.

The Onsager theory has been used with some success to describe the photoactivity of organic semiconductors such as anthracene [79, 80], naphthalene [81], poly(*N*-vinyl carbazole) [82], the poly(*N*-vinyl carbazole-trinitrofluorenone) charge transfer complex [83] and poly(9,6-di(*N*-carbazolyl)-2,4-hexadiyne) [84]. The validity of applying the Onsager theory is often checked by calculating the slope-to-intercept ratio $er_c/2kT$ in a plot of the carrier yield *versus* the electric field, using the low field approximation of eqn. (4). In anthracene it has been proposed that autoionization of the excited state brings about the initial electron–hole separation (*i.e.* the mechanism given in Section 4.1.1), and there is good agreement between the experimentally measured slope-to-intercept ratio and the theory.

However, the initial separation distance r_0 is treated as an adjustable parameter and no detailed theory of the initial charge separation has been developed. Also, the quantum efficiency of carrier generation in many organic thin films is wavelength independent and the photoconductivity or photovoltaic threshold coincides with the absorption threshold. These observations indicate that rapid relaxation in the excited state occurs before the carrier generation step. This presents a major difficulty in applying the original Onsager theory, especially as the principal mode of carrier formation in photovoltaic cells is thought to occur via exciton dissociation at dopant sites and not via autoionization. Noolandi and Hong [85] have attempted to overcome these difficulties by developing a model in which carrier generation proceeds in two steps after vibrational relaxation of the exciton.

In the first step, carriers are separated to a nearest-neighbour distance assumed to be equal to the average distance between molecules. This step is expected to be field dependent. In the second step, free electron–hole pairs are created by diffusion and drift in the electric field. However, Popovic and Menzel [86] found that both the original Onsager and the modified Noolandi–Hong theories failed to reproduce their data obtained for field-induced fluorescence quenching of dispersions of metal-free X- and β-phthalocyanine and 2-methoxy-5′-nitrophenylazo-2-naphthol-3-phenylcarboxamide in a polymer. They prefer a model in which the rate constant $k(F)$ for carrier production is an exponential function of the applied electric field, *i.e.*

$$k(F) = k_0 \exp\left(\frac{eaF}{kT}\right) \tag{5}$$

The carrier generation efficiency is then expressed as follows:

$$\eta(F) = \frac{k(F)}{k(F) + \Sigma k} \tag{6}$$

where Σk is the sum of all the decay rate constants of the singlet state, excluding carrier generation routes. Good experimental fits to a combination of these two expressions led the present authors to suggest that the parameter a is the jump distance of an electron in the primary photogeneration step and that eaF is an energy change, *i.e.* a lowering of the activation energy barrier to the electron jump, associated with the presence of the external electric field. This implies that the primary charge separation is the slow step in carrier production and that dissociation of the ion pair proceeds with unit efficiency after the initial charge separation.

In a recent paper by Yokoyama *et al.* [77], however, the Onsager theory predicted the temperature dependence and field-induced exciplex fluorescence quenching of a poly(*N*-vinyl carbazole) film doped with dimethylterephthalate, a weak electron acceptor. A thermalization distance of 22 Å gave the best fit. This distance was identified with the interionic separation of the electron–hole pair via a non-relaxed exciplex state produced from the interaction between a migrating singlet exciton and the electron acceptor. Their complete scheme is given as follows:

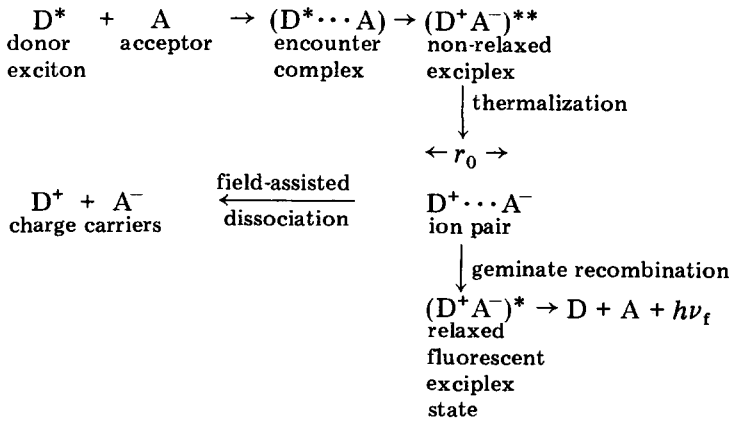

The temperature dependence was attributed to the thermal activation required to dissociate the thermalized ion pair, rather than being associated with the initial electron transfer step as in the Popovic and Menzel model.

The thermalization process from the non-relaxed exciplex state involves an increase in the interionic separation to r_0 as the excess energy dissipates. This may be envisaged as hole hopping from site to site in the ground-state levels of D (carbazole).

Additional support for the model came from experimental confirmation of the prediction that the fluorescence quenching should increase with the acceptor electron affinity. The model implied that increasing the electron affinity should lower the $D^+ \cdots A^-$ ion pair potential energy curve relative to that of the $D^* \cdots A$. Thus a greater excess of energy has to be dissipated during thermalization, resulting in an increase in r_0 with acceptor electron affinity, as observed.

In organic solar cells there is an additional recombination mechanism which manifests itself as a decrease in quantum yield with an increase in the absorbed light intensity. The photocurrent at short circuit does not increase proportionally with the light intensity but increases instead according to a power law of the type $I_{sc} \propto I_0^{\gamma}$ where γ ranges from 1 to 0.5. This dependence, which has also been observed in some inorganic devices, has been attributed to the presence of a high density of traps in the film. In illuminated p-type organic semiconductors the majority carrier (hole) lifetime τ_p is determined by the density of photogenerated electrons n by

$$\tau_p = \frac{1}{k_r n}$$

and (7)

$$\tau_n = \frac{1}{k_r p}$$

where k_r is a rate constant for recombination. In the presence of a high density of electron traps the steady state concentration n of electrons in the film increases and the hole lifetime is reduced. The increase in the recombination rate of electrons is n/τ_n. In the steady state, and when recombination is a significant loss process, the recombination rate must equal the generation rate I_0. Therefore, $I_0 = n/\tau_n$. Since the number of photogenerated electrons must equal the extra number of holes, then $I_0 = k_r n^2$ or $n \propto I_0^{0.5}$. The photocurrent is proportional to n, so $I_{sc} \propto I^{0.5}$. Reducing the rate of recombination depends on improving the photoconductivity by reducing the density of electron traps and increasing the electron mobility. A significant advance in improving the sunlight conversion efficiency has been the development of doped merocyanine films in which the photocurrents are linear in light intensity up to solar illumination levels [22, 36].

Until the dynamics of carrier generation in organic materials is understood and the generality of theoretical models is verified, it will be difficult to predict exact upper limits for J_{sc} and V_{oc} in photovoltaic cells. Ideally, the

models should also relate the efficiency to host and dopant molecular structures and the degree of film crystallinity. As we have seen, however, sufficient data are now available on the behaviour of organic semiconductors and photovoltaic cells to justify the formulation of a relatively simple model. This model has given useful insight in providing guidelines for the improvement of the photovoltaic efficiency by molecular engineering and is discussed in the following section.

6. Molecular structure and photovoltaic efficiency

The photovoltaic behaviour can be explained by means of the box diagram in Fig. 3 and the energy diagram in Fig. 4. During photoexcitation of the organic layer, excitons are created. The excitons (singlet or triplet)

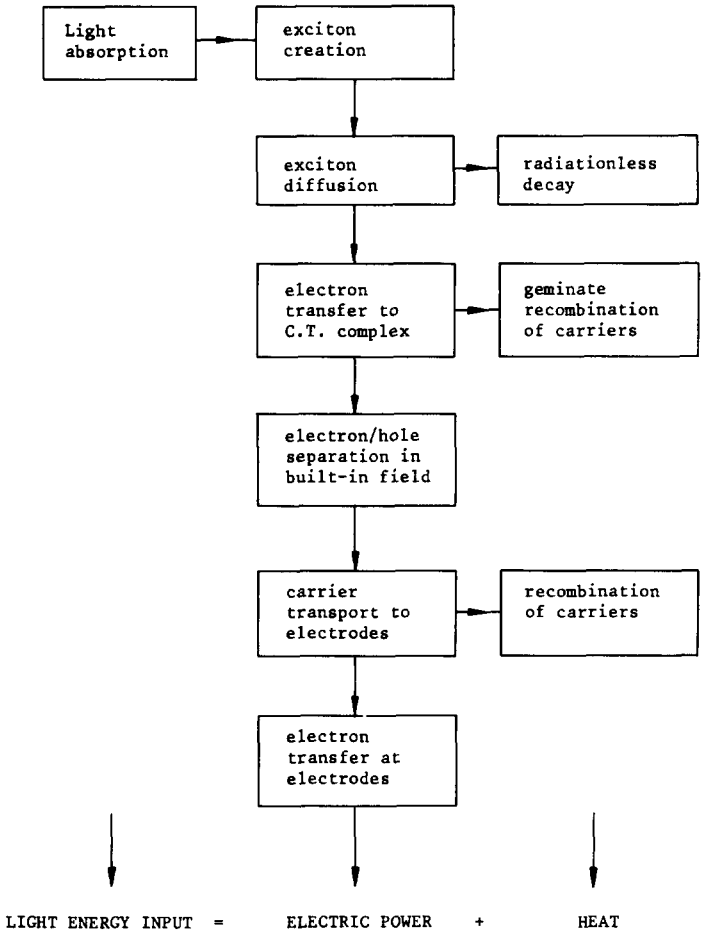

Fig. 3. Mechanism of photovoltaic behaviour.

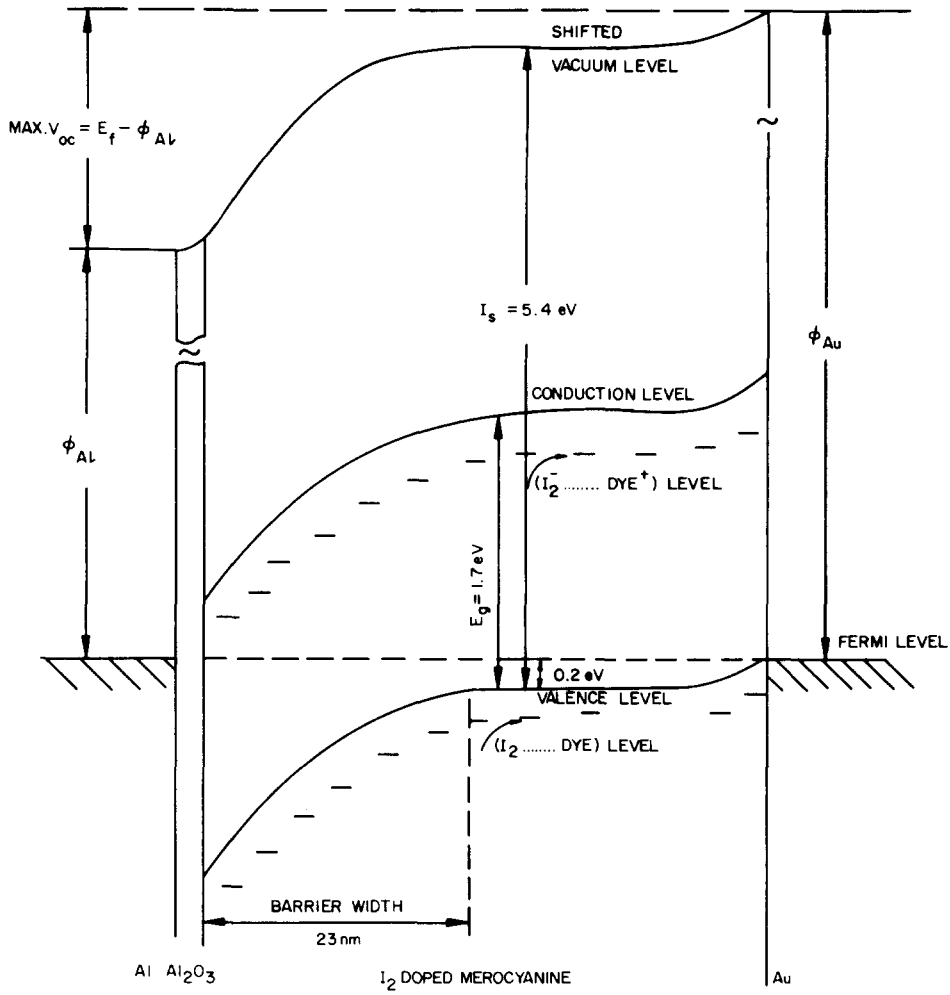

Fig. 4. Energy level diagram illustrating the photovoltaic effect in an iodine-doped merocyanine cell (Fig. 2, 9).

diffuse by hopping until they decay unimolecularly or transfer an electron to the lowest unoccupied molecular orbital of an organic compound–dopant charge transfer complex. The electron on the complex and the hole in the highest occupied molecular orbital of the organic compound can either undergo geminate recombination or dissociate in the built-in field region. This field region forms naturally in the vicinity of the barrier metal–organic interface by equalization of the chemical potentials. The photogenerated electrons and holes constitute a negative and a positive space charge respectively. The photocurrent is then limited by the drift of this space charge by electron hopping to the appropriate electrodes under the influence of the built-in field.

The quantum yield ϕ_ϵ of electron flow (*i.e.* the number of electrons flowing at short circuit per photon absorbed) can be written as

$$\phi_\epsilon = \phi_{ons}\phi_c \tag{8}$$

where ϕ_c is the efficiency of electron transfer to the electrode in the presence of recombination. ϕ_{ons} contains the term ϕ_0 (see eqn. (4)) which can be written as

$$\phi_0 = \frac{k_d[\text{M}\cdots\text{dopant}]}{k_d[\text{M}\cdots\text{dopant}] + \Sigma k} \tag{9}$$

where k_d is the rate constant for electron transfer from an exciton to an (M···dopant) complex site (*i.e.* the rate constant for the generation of thermalized ion pairs in the Onsager model). Thus it follows that ϕ_0 becomes larger as the concentration of the (M···dopant) complex increases. If [M··· dopant] becomes too large, however, then a substantial fraction of light will be absorbed by the complex. This is physically equivalent to the formation of excited complexes by mechanism (3) which is thought to be an inefficient way of generating carriers, so the overall efficiency is expected to decrease. It follows that there should be an optimum dopant concentration, but this point will not be considered further here.

The stability of a donor–acceptor complex in the ground state depends on its energy ΔE_N of formation and to a first approximation is proportional to $\exp(\Delta E_N/kT)$. From the simplified potential energy diagram of a complex shown in Fig. 5, we see that $\Delta E_N = W_N - I_s$ which implies that the stability of a series of complexes should increase as the ionization potential of the donor is reduced, provided that W_N remains at the same energy for a related series of complexes. As the complexes become more stable, a greater amount of dopant is trapped in the film. The problem then is to relate the ionization potential to the molecular structure so that efficient compounds may be prepared. This approach has been adopted and applied to the merocyanine class of dyes.

A considerable amount of work has been carried out on the merocyanines because of their photographic sensitizing properties [87], their photochromic behaviour [88] and their interesting solvent effects [87]. The merocyanines are neutral polymethine dyes in which an electron–donor group is linked to an electron–acceptor group by an unsaturated polymethine bridge. From a resonance point of view their true structure can be regarded as lying between a neutral form and a charge-separated form. It follows that the effective strengths of the donor group and acceptor group and the bridge length determine, amongst other properties, the ground and excited state polarities, the oxidation and reduction potentials (and hence the ionization potential and electron affinities respectively) and the wavelength λ_{max} of maximum absorption of the first electronic transition. Only the combination of a strong donor group and a weak acceptor group will result in a dye of low ionization potential. Therefore, we have carried out [34, 36] a study of the relationship between the photovoltaic activity of

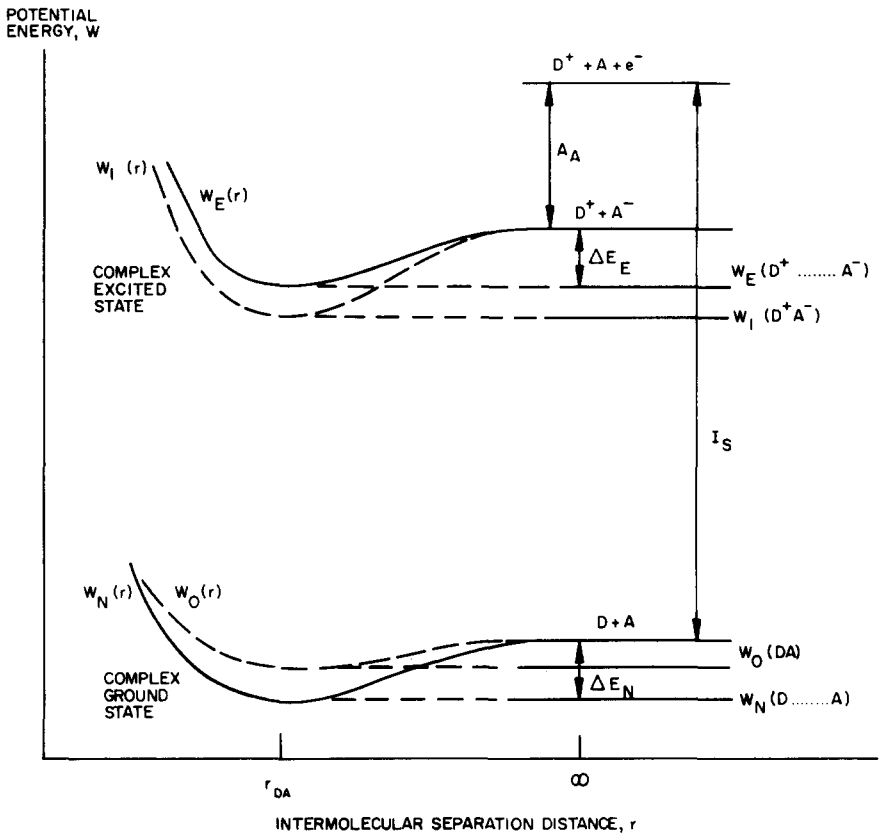

Fig. 5. Schematic diagram of the potential energy W of a DA complex against the intermolecular separation distance r: $W_N(r)$, (D···A) complex ground state; $W_E(r)$, ($D^+ \cdots A^-$) complex excited state; $W_0(r)$, DA structure; $W_I(r)$, D^+A^- structure; W_N, W_E, W_0, W_I, potentials at equilibrium separation; $r_{DA}I_S$, donor ionization potential; A_A, acceptor electron affinity (stability of (D···A) complex $\propto \exp\{(W_N - I_S)/kT\}$).

iodine-doped merocyanines and the molecular structure by systematically varying the donor and acceptor groups. The results are plotted in the form $\log \phi_\epsilon$ *versus* I_s in Fig. 6, as suggested by the dependence of complex stability (and hence concentration in our experimental conditions) on $\exp(\Delta E_N/kT)$ in Fig. 5. A reasonably good correlation was observed which has enabled us to prepare solar cells with efficiencies approaching 1%, using the more efficient dyes.

The effect of bridge length was investigated by comparing the response of compounds **9** and **10** in Fig. 2. The complete absence of a photovoltaic effect was recorded for the dye in which the donor group was directly attached to the acceptor group [36]. The result was interpreted in terms of the reduction in lifetime of the excited state caused by an out-of-plane twisting of the donor and acceptor groups to relieve the steric strain. Merocyanines of low I_s which contain more than two carbon atoms in the bridge tend to decompose when evaporated.

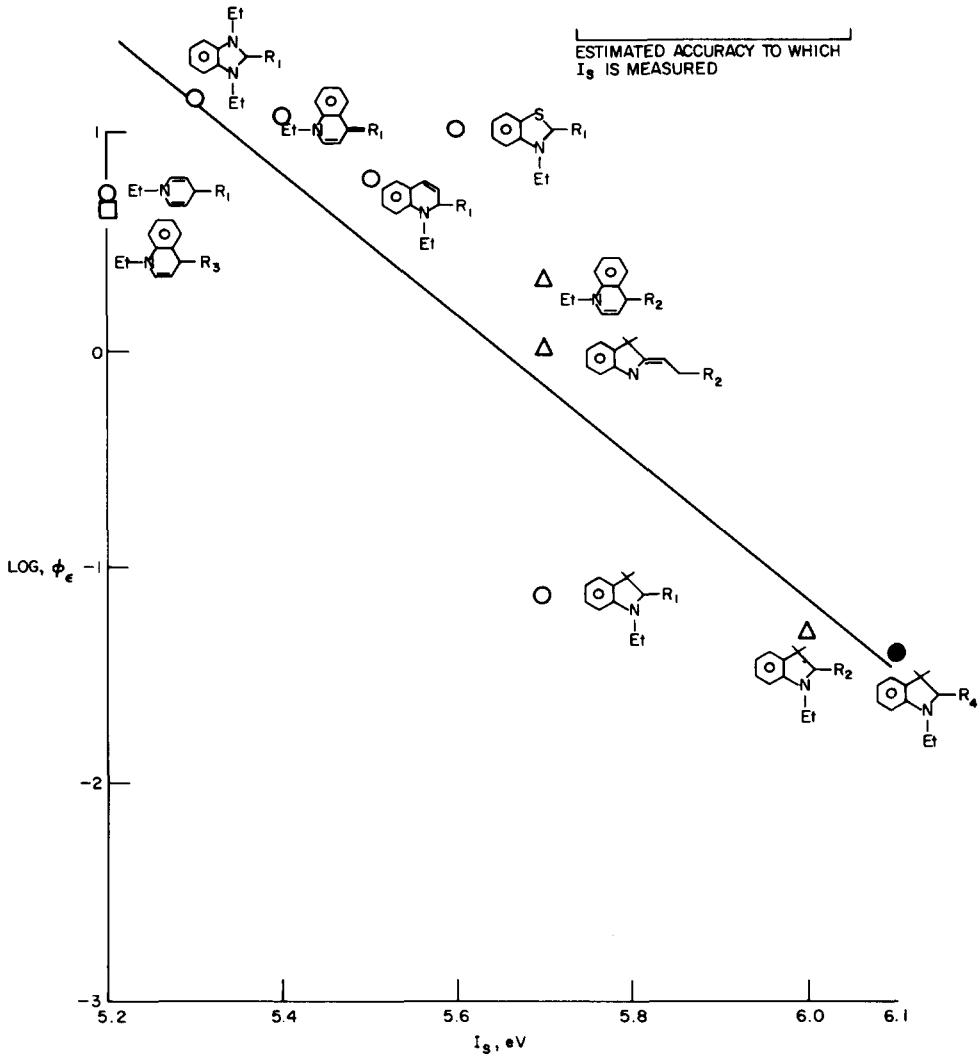

Fig. 6. Relationship between the quantum yield and the ionization potential for a series of merocyanine dyes

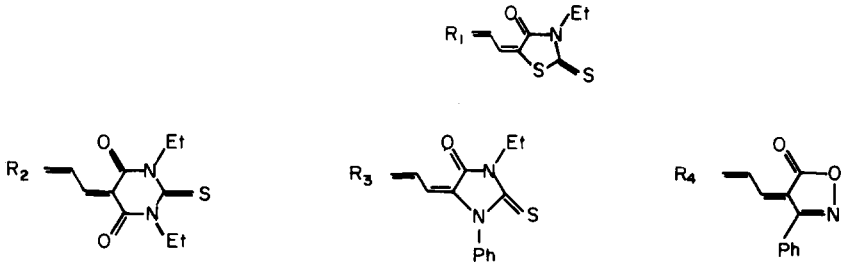

A similar correlation between the oxidation potential and $\log \phi_\epsilon$ was observed by Fajer and coworkers [28, 89] in liquid-junction porphyrin photovoltaic cells. Charge carrier formation in porphyrins is thought to proceed via oxygen complexes [90].

Some interesting results have been published recently [91 - 94] on the fluorescence quenching of a porphyrin (donor) residue by chemically attached quinone (acceptor) groups. For example, the fluorescence quantum yield ϕ_F and lifetime τ_s of *meso*-tetraphenylporphyrin are 0.13 ns and 15.7 ns respectively in benzene solution. If a phenyl group is replaced by quinone, ϕ_F drops by a factor of 19 and τ_s by 6.3 [93]. The fluorescence quenching is believed to occur by electron transfer from the porphyrin to the quinone. In a series of elegant experiments, Bolton and coworkers [95] have confirmed this by detecting the biradical $(\text{porphyrin})^{+\cdot}$–$(\text{quinone})^{-\cdot}$ in high yield under steady state conditions by electron paramagnetic resonance (EPR) spectroscopy on a related compound. It is possible that intramolecular donor–acceptor compounds of the type used by Bolton could show large quantum yields in organic cells.

7. Theoretical aspects of photovoltaic energy conversion and photocurrent modelling

The photovoltaic effect arises if two conditions are met. First, there must be a mechanism for the production of charge carriers by the action of light on an absorbing organic compound, as discussed. Secondly, the carriers have to be separated by a built-in electric field and to be collected at opposite electrodes. By analogy with ideal metal–semiconductor Schottky diodes [96], the built-in field is assumed to arise by electron diffusion during the equalization of the Fermi energies at the barrier metal–organic semiconductor contact. By the depletion layer approximation, the field $F_s(x)$ in the semiconductor depletion region is given by

$$F_s(x) = \frac{eN_a}{\epsilon_s \epsilon_0}(x - w) \tag{10}$$

and the potential drop V_{bi} across the depletion layer is given by

$$V_{bi} = \int_0^w F_s(x)\,dx = \frac{eN_A w^2}{2\epsilon_s \epsilon_0} \tag{11}$$

where N_A is the acceptor density responsible for the dark semiconductivity of the organic material, ϵ_s is the semiconductor permittivity, ϵ_0 is the vacuum permittivity, w is the width of the depletion region and x is measured from the contact towards the semiconductor bulk. Table 4 shows the depletion layer characteristics for some cells reported in the literature. In general, w is less than 500 Å because of the large number of defect sites which act as ionizing centres. The depletion layer width has been determined

TABLE 4

Depletion layer and diode characteristics of some organic photovoltaic cells

Cell	w (Å)	V_{bi} (V)	N_A (cm^{-3})	J_0[a] ($A\ cm^{-2}$)	n[b]	N_T (cm^{-3})	*Reference*
Phthalocyanines							
(1) In/X-H_2Pc in polymer/NESA	300, C	0.63	3×10^{17}	3×10^{-9}	1.3 - 2.6	6×10^{16}	[31]
(2) Al/X-H_2Pc in polymer/NESA	320, C 380, A	≈0.9	3×10^{17}	1.23×10^{-9}	1.77		[24]
(3) Al/H_2Pc/Au						$\approx 10^{19}$	[7]
(4) In/H_2Pc/Au				1.77×10^{-10}	1.5	$\approx 10^{19}$	[7]
(5) In/ZnPc/Au				3.5×10^{-8}	1.37	$\approx 10^{18}$	[7]
(6) Al/MgPc/Ag	200 - 250, C 250, A	0.62	$(0.8 - 1.4) \times 10^{18}$				[13]
(7) Al/MgPc/Ag	300 - 500, C	0.7	$\approx 10^{19}$				[97]
(8) Al/CuPc/Ag	800, C	0.64	2×10^{16}			$\approx 10^{16}$	[98]
(9) Al/CuPc/Au	250, A					$\approx 10^{18} - 10^{19}$	[99]
Merocyanines							
(1) Al/merocyanine/Ag	400 - 500, C	1.1 - 1.6	$(2 - 5) \times 10^{17}$				[100]
(2) Al/merocyanine/Au	230, C	1.05	$\approx 10^{18}$				[35]
(3) n-TiO_2/merocyanine/Au			$\approx 10^{17}$				[27]
Others							
(1) Al/tetracene/Au or NESA	2000, C	≈1.2	$\approx 10^{16}$				[101]
(2) Al/tetracene/Au						7×10^{19}	[12]
(3) Cr/chlorophyll-a/Hg				2×10^{-11}	1.6		[15]
(4) Al/CH_x, HCl doped/Au		1.1					[30]

A, determined from action spectra; C, determined from capacitance.

[a] Reverse saturation current.

[b] Diode quality factor.

experimentally by two methods, the capacitance method and the action spectra method. In the capacitance method, w is obtained from the value of the differential capacitance at zero bias in a plot of $1/C^2$ *versus* the applied voltage at low frequency. At high frequencies, *i.e.* greater than 100 Hz, the capacitance becomes voltage independent for merocyanine cells [35]. A similar observation has been made on illuminated tetracene cells at frequencies above about 1 Hz [101]. The results for tetracene were explained in terms of a model in which the depletion layer is formed from a high density of immobile trapped charge which can be mobilized by illumination.

In the action spectra method, several researchers working with different organic dyes have noticed a difference in the action spectrum obtained when light is incident on the barrier side compared with the response obtained when light is incident on the ohmic contact side. For front illumination the strongly absorbed light creates excited states in the depletion region. Under these conditions, the absorption spectrum is usually well matched to the action spectrum. For back illumination the organic material itself acts as a filter of the strongly absorbed light in the field-free bulk region and only weakly absorbed photons at the sides of the absorption peaks penetrate to the depletion region and make a major contribution to the photocurrent. An example of this behaviour is given in Fig. 7. The spectral response is then some function of the reciprocal of the absorption coefficient. The depletion layer width can thus be estimated provided that the exciton diffusion length is known, but the value obtained will depend on the particular model used to predict the photocurrent response.

Modelling the photovoltaic behaviour of organic cells usually begins by solving the diffusion equation of excitons in the steady state, *i.e.*

$$D\frac{d^2c}{dx^2} - kc + \alpha I_0 \exp(-\alpha x) = 0 \tag{12}$$

where D is the one-dimensional diffusion coefficient of excitons, c is the concentration of excitons at a given plane at a distance x from the metal–organic interface (where $x = 0$), k is the total annihilation rate constant for excitons, α is the absorption coefficient and I_0 is the flux density of unreflected monochromatic photons entering the organic film.

A number of boundary conditions are possible, *e.g.* at $x = 0$, $c = 0$ or $D(dc/dx) = sc(0)$, where s is the surface recombination velocity, at $x = d$ (where d is the thickness of the organic film), $c = 0$ and at $x = \infty$, $c = 0$. The most realistic conditions appear to be $c = 0$ at $x \approx 0$ and $x = d$ because of the rapid quenching of excitons by metals. The exciton distribution is then given by

$$c(x) = \frac{I_0\alpha}{k(1-\alpha^2L^2)}\left[\exp(-\alpha x) + \frac{\exp(x/L)}{\exp(d/L) - \exp(-d/L)}\left\{\exp\left(-\frac{d}{L}\right) - \exp(-\alpha d)\right\} - \frac{\exp(-x/L)}{\exp(d/L) - \exp(-d/L)}\left\{\exp\left(\frac{d}{L}\right) - \exp(-\alpha d)\right\}\right] \tag{13}$$

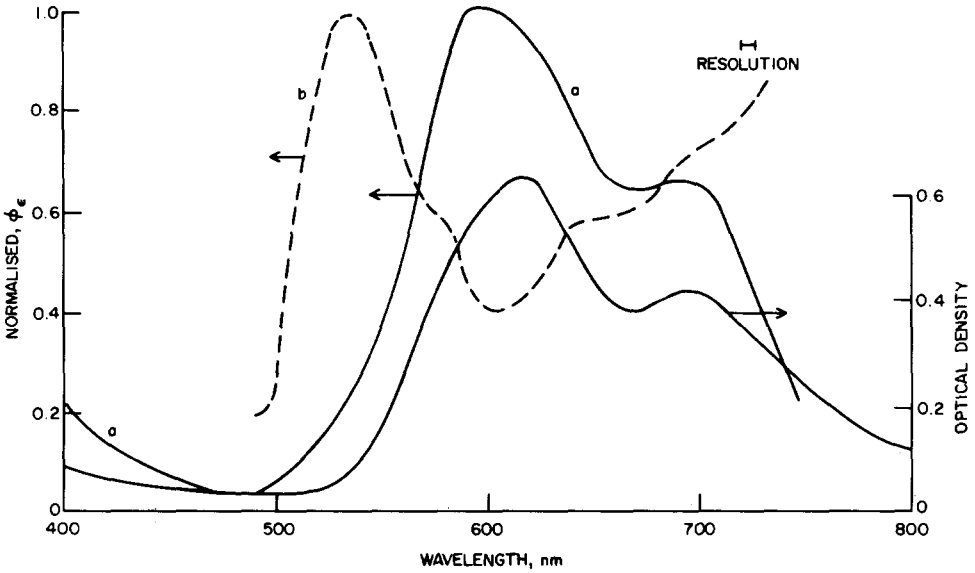

Fig. 7. Absorption spectrum of copper phthalocyanine (60 nm thick) and variation in quantum yield with excitation wavelength for illumination through aluminium (curve a) and gold (curve b).

where L is the exciton diffusion length ($L = (D/k)^{1/2}$).

Ghosh and Feng [22] have assumed that free carriers are generated only if excitons reach the front electrode in aluminium–merocyanine cells. The exciton current J_{Al} for front illumination is then given by

$$J_{Al} = -D \left.\frac{dc}{dx}\right|_{x=0} \tag{14}$$

$$= -\frac{\alpha I_0}{\alpha + 1/L} \qquad \text{if } \exp\left(-\frac{d}{L}\right) \ll 1 \tag{15}$$

The photocurrent can be expressed as

$$J_L = \frac{eI_0\phi\alpha}{\alpha + 1/L} \tag{16}$$

and the quantum yield based on the incident light is then given by

$$\phi_i = \frac{\phi\alpha}{\alpha + 1/L} \tag{17}$$

where ϕ is the exciton dissociation efficiency for carrier generation.

However, if carrier generation is a bulk phenomenon in which carriers are created at dopant sites of concentration N_d as discussed previously, then a different expression for the quantum yield ϕ_i is obtained. The generation rate of carriers at x is $k_d N_d c(x)\phi_{esc}(x)$. In the Onsager model, k_d can be identified with the rate constant for the generation of thermalized ion pairs

and $\phi_{esc}(x)$ with the efficiency of escape of the opposite charges from their mutual coulombic attraction. On the assumption that only carriers that are created in the depletion layer contribute to the photocurrent and that there is no recombination, the photocurrent is given by

$$J_{ph} = e\int_0^w k_d N_d \phi_{esc}(x) c(x)\, dx \tag{18}$$

The upper limit for the photocurrent is then determined by the fraction of incident light that is absorbed in the depletion region and by the diffusion length of excitons, on the assumption that $\phi_{esc} = 1$ for $0 < x < w$. Substituting for $c(x)$ and performing the integration, we obtain

$$J_{ph} = \frac{eI_0 k_d N_d}{k(1-\alpha^2 L^2)}\left(1 - \exp(-\alpha w) + \right.$$
$$+ \frac{\alpha L[\{\exp(w/L) - 1\}\{\exp(-d/L) - \exp(-\alpha d)\}]}{\exp(d/L) - \exp(-d/L)} -$$
$$\left. - \frac{\alpha L[\{1 - \exp(-w/L)\}\{\exp(d/L) - \exp(-\alpha d)\}]}{\exp(d/L) - \exp(-d/L)}\right) \tag{19}$$

The quantum yield based on the incident light is then

$$\phi_i = \frac{J_{ph}}{eI_0} \tag{20}$$

In eqn. (19), k is equal to $k_d N_d + \Sigma k$ and therefore $k_d N_d/k$ is the efficiency ϕ_0 of exciton dissociation. In Fig. 8, ϕ_i/ϕ_0 *versus* w is plotted for different values of α and L. It is apparent that for a typical depletion layer width of about 300 Å the upper limit for ϕ_i/ϕ_0 is between 50% and 60% for strongly absorbed light ($\alpha \approx 3 \times 10^5$ cm^{-1}). If $\phi_0 \approx 1$, then $\phi_i \approx 60\%$ is the upper limit for the quantum yield (on the basis of the light incident on the organic film) at the peak absorption wavelength of the organic material. The average upper limit of ϕ_i over the absorption spectrum will be considerably less than 60% because of the highly structured absorbances of organic compounds. By extending this argument further, we can calculate the upper limit for the short-circuit photocurrent J_{sc} for a promisingly efficient merocyanine dye (Fig. 2, 9) illuminated by air mass (AM) 1 sunlight.

$$J_{sc}(\max) = \int_{\lambda_2}^{\lambda_1} J_{ph}(\lambda)\, d\lambda$$
$$= 6.6 \text{ mA cm}^{-2} \tag{21}$$

The parameter values used in this calculation are w = 230 Å, L = 0, d = 500 Å, the absorption spectrum given in ref. 36, the AM 1 solar spectrum given in ref. 102, λ_1 = 390 nm and λ_2 = 800 nm. The upper limit

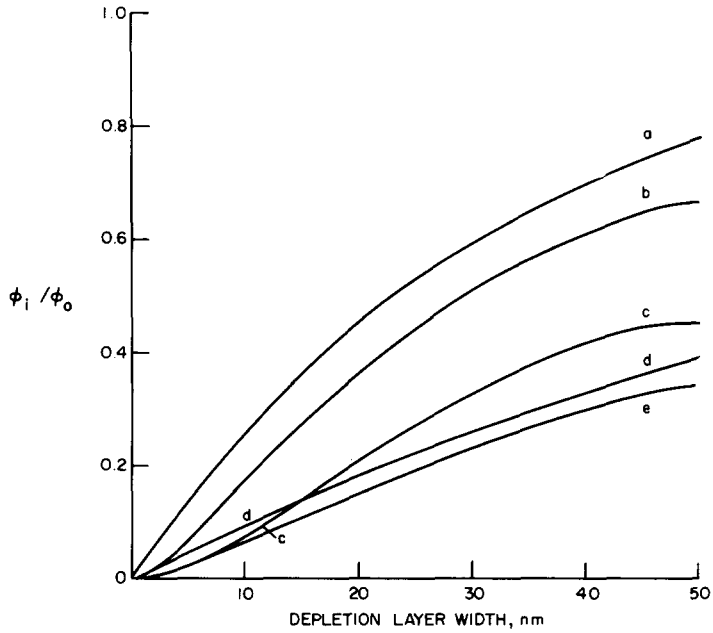

Fig. 8. Plot of ϕ_i/ϕ_0 based on incident light *vs.* depletion layer width: curve a, $\alpha = 3 \times 10^5$ cm^{-1}, $L = 0$ nm; curve b, $\alpha = 3 \times 10^5$ cm^{-1}, $L = 3$ nm; curve c, $\alpha = 3 \times 10^5$ cm^{-1}, $L = 10$ nm; curve d, $\alpha = 1 \times 10^5$ cm^{-1}, $L = 0$ nm; curve e, $\alpha = 1 \times 10^5$ cm^{-1}, $L = 3$ nm.

on ϕ_i averaged over this range of wavelengths was calculated to be 0.25. This calculation highlights the large losses arising from poor matching of the absorption and solar spectra and the short depletion length. In order to increase J_{sc}(max), the absorber must be tailored to absorb strongly over the entire visible spectrum up to about 900 nm. Alternatively, multilayers of single absorbers may suffice, but interface recombination effects are highly probable. Another approach is to increase w by identifying and reducing the density N_A of acceptor states. In order to offset the loss in electrical conductivity ($\sigma = e\mu p \approx e\mu N_A^-$ where N_A^- is the density of negatively charged acceptors), the charge mobility μ must be increased by at least a proportional amount. This may be achieved by improving the film crystallinity and purity.

Yet another approach would be to prepare an organic p–n junction by interfacing a p-type dye, such as a merocyanine, with an n-type dye, such as a triphenylmethane. The light absorption property of the cell would be substantially improved by such an arrangement. Kudo and Moriizumi [103] recently demonstrated the feasibility of this approach by extending the earlier work of Meier [3]. They prepared an ITO/malachite green/merocyanine 5/Ag cell with a sunlight conversion efficiency of 0.05%.

8. Sunlight conversion efficiency, η_s

The theoretical maximum sunlight conversion efficiency of organic cells is of considerable interest if practical devices are to be developed. The efficiency of any optoelectronic converter is given by

$$\eta_s = \left(JV \Big/ \int_0^{E_{max}} EN(E)\, dE \right) \times 100\% \tag{22}$$

The equation is more useful if it is expressed [104 - 106] as the product of a number of dimensionless groups each of which refers to an energy dissipation process in the cell, *i.e.*

$$\eta_s = (1 - R) \frac{E_g \int_{E_g}^{E_{max}} N(E)\, dE}{\int_0^{E_{max}} EN(E)\, dE} \frac{eV_{oc}}{E_g} \frac{J_{sc}/e}{(1 - R) \int_{E_g}^{E_{max}} N(E)\, dE} \frac{JV}{J_{sc} V_{oc}} \tag{23}$$

= reflection losses × light absorption efficiency × voltage factor × × average quantum yield × fill factor

In this equation, R is the ratio of the reflected to the incident energies, E_g is the threshold energy of absorption and $N(E)$ is the flux density of incident photons per unit energy interval. For a "perfect" device with an E_g of 1.4 eV at room temperature the efficiency in AM 1 sunlight is

$$\eta_s = 1 \times 0.44 \times 0.7 \times 1 \times 1$$
$$= 31\%$$

The value of 0.7 for the voltage factor arises from constraints due to the second law of thermodynamics (see for example refs. 107 - 109).

In practice, there are losses due to reflection, current collection and resistance which limit η_s to about 23%. In a single-threshold absorbing organic cell there are additional losses arising from the field-dependent quantum efficiency and poor matching of the absorption and solar spectra. Let us consider the merocyanine cell discussed previously. If we assign "best" estimates to each of the terms, the ultimate efficiency for this cell with no reflection loss will be

$$\eta_s \approx 1 \times 0.4 \times \frac{1}{1.55} \times 0.25 \times 0.6 \approx 4\%$$

This should be compared with

$$\eta_s = \frac{I_{sc} V_{oc} FF}{I_0} = \frac{6.6\ \text{mA} \times 1.0\ \text{V} \times 0.6}{900\ \text{mW}} = 4.4\%$$

An analysis of the loss processes in an experimentally measured sunlight efficiency for the cell Al/merocyanine, Cl_2 doped/Au led to the following:

$$\eta_s(\text{measured}) = 0.6 \times 0.4 \times \frac{0.74}{1.55} \times 0.08 \times 0.39 = 0.36\%$$

In the calculation of the ultimate efficiency a fill factor of 0.6 has been optimistically assumed to be within reach, although in practice values between 0.3 and 0.44 are often measured. The development of better models should quantify the fill factor more rigorously. In contrast, Tang *et al.* [10, 11] have reported a fill factor of 0.6 in a CuPc/perylene cell.

The result strongly suggests that an organic cell based on a single-threshold absorber with a typical depletion layer width of 230 Å will not be efficient enough for solar photovoltaic energy conversion on a large scale. However, by broadening the absorption spectrum and extending the depletion layer width to 500 Å, an ultimate efficiency of about $1 \times 0.44 \times 0.7 \times 0.7 \times 0.6$ or 13% is obtained. The problems in achieving this efficiency in practice are formidable but not entirely out of the question. For example, Loutfy *et al.* [31] recently measured a monochromatic quantum yield ϕ_i of 45% based on 600 nm light incident on an X-H_2Pc in polymer film at low light level. This value is close to the upper limit of 63% at w = 300 Å and $\alpha = 3.3 \times 10^5$ cm^{-1} in Fig. 8. In this cell it is interesting that the barrier width is greater than in the equivalent evaporated X-H_2Pc continuous films. If recombination, reflection and absorption losses can be overcome, then this cell will be highly efficient in sunlight.

9. Stability of organic cells

A major problem with organic devices is their instability, especially at high light intensities; however, the mode of degradation and the time evolution of photoresponse have received little attention. The published data, summarized in Tables 1 and 2, suggest that the following processes contribute to the photocurrent decay in organic cells: (a) the build-up of oxide layers on the barrier metal surface; (b) photodegradation (UV and visible) and thermal degradation of the dye.

In principle, process (a) can be minimized by encapsulation and similarly process (b) may be reduced if molecular oxygen (singlet molecular oxygen reactions with organic materials are extensively reported) is involved. However, it is possible that the degradation of the organic layer may proceed via isomerization and other rearrangements [34, 88, 110, 111]. In this case, introducing substituents that block the rearrangement, or just making the photovoltaic steps more efficient at the expense of rearrangement, may stabilize the organic material. A simple calculation reveals that in order to meet the requirements for long-term stability (5 years) the quantum yield of photodegradation processes should be less than 10^{-6}% on the assumption that a 10% loss in photocurrent can be tolerated.

Future investigations will reveal whether or not organic cells will meet the stringent efficiency and stability requirements necessary for practical devices.

10. Summarizing remarks

The status of organic solar cells has been reviewed. The research is still in its early stages, but efficiencies approaching 1% in sunlight have been reported. Their photoelectric and rectifying behaviour bear some resemblance to conventional Schottky barrier or MIS devices, but the ultimate efficiency is constrained to lower values by the field-dependent quantum efficiency, short depletion widths, poor matching of absorption spectra with the solar spectrum and series resistance. Some of these problems can be overcome, however, by molecular tailoring of the organic material, by reducing the high density of trap sites and by molecular doping.

A review of doping effects in photoconductivity and photovoltaic cells has emphasized that molecular doping is crucial for efficient carrier photogeneration. The mechanism is thought to involve the formation of charge transfer complexes at specific sites in the bulk of the organic film. Future progress will depend on optimizing the type, concentration and distribution of dopant in the organic film.

Theoretical models of photovoltaic response are still in an early stage of development. However, the results from photocurrent efficiencies and field-dependent fluorescence quenching in photoconductivity cells should find some application, especially Onsager's theory of geminate recombination. Once the validity of such models has been tested, it should be possible to predict the limiting photocurrents, open-circuit voltages and fill factors and hence the efficiencies of cells containing promising classes of organic compounds such as the phthalocyanines and merocyanines. In this review, an ultimate efficiency of only about 4% is predicted for a merocyanine cell in which the barrier width is 23 nm. However, if the absorption spectrum is broadened, *e.g.* by photosensitization or by molecular tailoring, and the barrier width is extended, then efficiencies of around 10% should be within reach.

References

1 F. Gutmann and L. E. Lyons, *Organic Semiconductors*, Wiley, 1967, Chap. 8, p. 516.
2 H. Kallmann and M. Silver (eds.), *Symposium on Electrical Conductivity in Organic Solids*, Wiley-Interscience, New York, 1961, pp. 39, 69, 291.
3 H. Meier, *Organic Semiconductors*, Chemie, Weinheim, 1974, p. 370.
4 J. Shewchun, R. Singh and M. A. Green, *J. Appl. Phys.*, *48* (1977) 765.
5 M. A. Green, F. D. King and J. Shewchun, *Solid-State Electron.*, *17* (1974) 551.
6 H. J. Hovel, *Semiconductors and Semimetals*, Vol. 11, *Solar Cells*, Academic Press, New York, 1975.
7 F. R. Fan and L. R. Faulkner, *J. Chem. Phys.*, *69* (1978) 3334.

8 C. K. Hsiao, R. O. Loutfy and J. H. Sharp, Solar energy — bringing it down to earth, *U.S. DOE Rep. CONF-7908116*, Vol. 2, 1979, pp. 79 - 104 (U.S. Department of Energy).
9 L. Holland, *Vacuum Deposition of Thin Films*, Chapman and Hall, London, 1961, p. 73.
10 C. W. Tang, A. P. Marchetti and R. H. Young, *U.S. Patent 4,125,414*, November 14, 1978.
11 C. W. Tang, *U.S. Patent 4,164,431*, August 14, 1979.
12 A. K. Ghosh and T. Feng, *J. Appl. Phys., 44* (1973) 2781.
13 A. K. Ghosh, D. L. Morel, T. Feng, R. F. Shaw and C. A. Rowe, Jr., *J. Appl. Phys., 45* (1974) 230.
14 C. W. Tang and A. C. Albrecht, *J. Chem. Phys., 63* (1975) 953.
15 C. W. Tang and A. C. Albrecht, *Nature (London), 254* (1975) 507.
16 V. Y. Merritt and H. J. Hovel, *Appl. Phys. Lett., 29* (1976) 414.
17 V. Y. Merritt, *IBM J. Res. Dev., 22* (1978) 353.
18 E. W. Williams, *Solid-State Electron Devices, 1* (1977) 185.
19 F. J. Kampas and M. Goutermann, *J. Phys. Chem., 81* (1977) 690.
20 F. R. Fan and L. R. Faulkner, *J. Chem. Phys., 67* (1978) 3341.
21 D. L. Morel, A. K. Ghosh, T. Feng, E. L. Stogryn, P. E. Purwin and C. Fishman, *Appl. Phys. Lett., 32* (1978) 495.
22 A. K. Ghosh and T. Feng, *J. Appl. Phys., 49* (1978) 5982.
23 V. A. Benderskii, M. I. Al'yanov, M. I. Federov and L. M. Federov, *Dokl. Akad. Nauk S.S.S.R., 239* (1978) 856.
24 R. O. Loutfy and J. H. Sharp, *J. Chem. Phys., 71* (1979) 1211.
25 A. F. Janzen and J. R. Bolton, *J. Am. Chem. Soc., 101* (1979) 6342.
26 P. J. Reucroft and H. Ullal, *Sol. Energy Mater., 2* (1979 - 1980) 217.
27 T. A. Skotheim, *Diss. Abstr. Int. B, 41* (1980) 257.
28 F. J. Kampas, K. Yamashita and J. Fajer, *Nature (London), 284* (1980) 40.
29 B. R. Weinberger, S. C. Gan and Z. Kiss, *Appl. Phys. Lett., 38* (1981) 555.
30 J. Tsukamoto, H. Ohigashi, K. Matsumura and A. Takahashi, *Jpn. J. Appl. Phys., 20* (1981) L127.
31 R. O. Loutfy, J. H. Sharp, C. K. Hsiao and R. Ho, *J. Appl. Phys., 52* (1981) 5218.
32 T. Moriizumi and K. Kudo, *Appl. Phys. Lett., 38* (1981) 85.
33 G. A. Chamberlain and P. J. Cooney, *Chem. Phys. Lett., 66* (1979) 88.
34 G. A. Chamberlain and R. E. Malpas, *Faraday Discuss. Chem. Soc., 70* (1980) 299.
35 G. A. Chamberlain, *J. Appl. Phys., 53* (1982) 6262.
36 G. A. Chamberlain, P. J. Cooney and S. Dennison, *Nature (London), 289* (1981) 45.
37 A. Nevin and G. A. Chamberlain, to be published.
38 J. Mort, *Science, 208* (1980) 819.
39 R. L. Van Ewyk, A. V. Chadwick and J. D. Wright, *J. Chem. Soc. Faraday Trans. 1, 76* (1980) 2194.
40 R. L. Van Ewyk, A. V. Chadwick and J. D. Wright, *J. Chem. Soc. Faraday Trans. 1, 77* (1981) 73.
41 Z. D. Popovic and J. H. Sharp, *J. Chem. Phys., 66* (1977) 5076.
42 G. A. Cox and P. C. Knight, *J. Phys. C, 7* (1974) 146.
43 E. R. Menzel and R. O. Loutfy, *Chem. Phys. Lett., 72* (1980) 522.
44 S. C. Dahlberg and M. E. Musser, *J. Chem. Phys., 72* (1980) 6706.
45 S. E. Harrison and K. H. Ludewig, *J. Chem. Phys., 45* (1966) 343.
46 J. Manassen, *Catal. Rev., 9* (1974) 223.
47 M. E. Musser and S. C. Dahlberg, *Surf. Sci., 100* (1980) 605.
48 S. C. Dahlberg and M. E. Musser, *Surf. Sci., 90* (1979) 1.
49 W. A. Orr and S. C. Dahlberg, *J. Am. Chem. Soc., 101* (1979) 2875.
50 S. L. Hsu, A. J. Signorelli, G. P. Pez and R. H. Baughman, *J. Chem. Phys., 69* (1978) 106.
51 I. Harada, Y. Furukawa, M. Tasumi, H. Shirakawa and S. Ikeda, *Chem. Lett.*, (1980) 267.

52 R. Bahri, R. K. Bali and B. R. Sood, *J. Phys. D, 13* (1980) L39.
53 H. Hoegl, *J. Phys. Chem., 69* (1965) 755.
54 J. K. Jeszka, J. Ulanski and M. Kryszewski, *Nature (London), 289* (1981) 390.
55 N. Karl, *Festkörperprobleme, 14* (1974) 261.
56 H. Baessler, H. Killesreiter and G. Vaubel, *Discuss. Faraday Soc., 51* (1971) 48.
57 H. Killesreiter and H. Baessler, *Chem. Phys. Lett., 11* (1971) 411.
58 G. Vaubel, H. Baessler and D. Mobius, *Chem. Phys. Lett., 10* (1971) 334.
59 H. Killesreiter and H. Baessler, *Phys. Status Solidi B, 51* (1972) 657.
60 H. Kallmann, G. Vaubel and H. Baessler, *Phys. Status Solidi B, 44* (1971) 813.
61 H. Killesreiter and H. Baessler, *Phys. Status Solidi B, 53* (1972) 193.
62 F. Funfschilling and D. F. Williams, *Chem. Phys. Lett., 31* (1975) 551.
63 W. Arden, M. Kotani and L. M. Peter, *Chem. Phys. Lett., 40* (1976) 32.
64 M. Silver, D. Olness, M. Swicord and R. C. Jarnagin, *Phys. Rev. Lett., 10* (1963) 12.
65 M. Schott and J. Berrehar, *Phys. Status Solidi B, 59* (1973) 175.
66 J. Fourny, G. Delacote and M. Schott, *Phys. Rev. Lett., 21* (1968) 1085.
67 R. G. Kepler, *Phys. Rev. Lett., 18* (1967) 951.
68 E. Courtens, A. Bergman and J. Jortner, *Phys. Rev., 156* (1967) 948.
69 P. Holzman, R. Morris, R. C. Jarnagin and M. Silver, *Phys. Rev. Lett., 19* (1967) 506.
70 R. G. Kepler, *Pure and Appl. Chem., 27* (1971) 515.
71 P. Petelenz, *Chem. Phys. Lett., 65* (1979) 579.
72 L. Onsager, *J. Chem. Phys., 2* (1934) 599; *Phys. Rev., 54* (1938) 554.
73 E. R. Menzel and Z. D. Popovic, *Chem. Phys. Lett., 55* (1978) 177.
74 E. R. Menzel and R. O. Loutfy, *Chem. Phys. Lett., 72* (1980) 522.
75 M. Yokoyama, Y. Endo and H. Mikawa, *Chem. Phys. Lett., 34* (1975) 597.
76 M. Yokoyama, Y. Endo and H. Mikawa, *Bull. Chem. Soc. Jpn., 49* (1976) 1538.
77 M. Yokoyama, Y. Endo, A. Matsubara and H. Mikawa, *J. Chem. Phys., 75* (1981) 3006.
78 D. M. Pai and R. C. Enck, *Phys. Rev. B, 11* (1975) 5163.
79 R. R. Chance and C. L. Braun, *J. Chem. Phys., 64* (1976) 3573.
80 R. H. Batt, C. L. Braun and J. R. Horning, *J. Chem. Phys., 49* (1967) 1967.
81 V. N. Joshi and M. Castillo, *Chem. Phys. Lett., 46* (1977) 317.
82 G. Pfister and D. J. Williams, *J. Chem. Phys., 61* (1974) 2416.
83 P. J. Melz, *J. Chem. Phys., 57* (1972) 1694.
84 K. Lochner, H. Bassler, L. Sebastian, G. Weiser, G. Wegner and V. Enkelmann, *Chem. Phys. Lett., 78* (1981) 366.
85 J. Noolandi and K. M. Hong, *J. Chem. Phys., 70* (1979) 3230.
86 Z. D. Popovic and E. R. Menzel, *J. Chem. Phys., 71* (1979) 5090.
87 J. Griffiths, *Colour and Constitution of Organic Molecules*, Academic Press, London, 1976, Chap. 6, p. 140.
88 R. C. Bertelson, in G. H. Brown (ed.), *Techniques of Chemistry*, Vol. 3, Wiley, London, 1971, Chap. 3.
89 K. Yamashita, K. Maenobe and J. Fajer, *Chem. Lett.*, (1980) 307.
90 A. T. Vartanyan, *Sov. Phys. — Semicond., 1* (1968) 1261.
91 J. Dalton and L. R. Milgram, *J. Chem. Soc., Chem. Commun.*, (1979) 609.
92 I. Tabushi, N. Koga and M. Yanagita, *Tetrahedron Lett., 3* (1979) 257.
93 A. Harriman and R. J. Hosie, *J. Photochem., 15* (1981) 163.
94 T. L. Netzel, M. A. Bergkamp, C.-K. Chang and J. Dalton, *J. Photochem., 17* (1981) 451.
95 T.-F. Ho, A. R. McIntosh and J. R. Bolton, *Nature (London), 286* (1980) 254.
96 S. M. Sze, *Physics of Semiconductor Devices*, Wiley-Interscience, New York, 1969, p. 370.
97 M. I. Federov and V. A. Benderskii, *Sov. Phys. — Semicond., 4* (1971) 1198.
98 B. S. Barkhalov and Yu. A. Vidadi, *Thin Solid Films, 40* (1977) L5.
99 G. A. Chamberlain, unpublished work, 1980.
100 K. Iriyama, M. Shiraki, K. Tsuda, A. Okada, M. Sugi, S. Iizima, K. Kudo, S. Shiokawa,

T. Moriizumi and T. Yasuda, *Jpn. J. Appl. Phys., 19* (1980) 173.
101 A. J. Twarowski and A. C. Albrecht, *J. Chem. Phys., 70* (1979) 2255.
102 C. Bachus (ed.), *Solar Cells*, IEEE, New York, 1976.
103 K. Kudo and T. Moriizumi, *Jpn. J. Appl. Phys., 20* (1981) L553.
104 M. D. Archer, *J. Appl. Electrochem., 5* (1975) 17.
105 M. D. Archer, *Sol. Energy, 20* (1978) 167.
106 H. D. Sharf, J. Fleischhauer, H. Leismann, I. Ressler, W. Schleker and R. Weitz, *Angew. Chem., Int. Edn. Engl., 18* (1979) 652.
107 W. Shockley and H. J. Queisser, *J. Appl. Phys., 32* (1961) 510.
108 R. T. Ross, *J. Chem. Phys., 46* (1967) 4590.
109 C. D. Mathers, *J. Appl. Phys., 48* (1977) 3181.
110 V. A. Kuz'min, A. M. Vinogradov, N. N. Romanov, M. A. Al'perovich, I. I. Levokev and F. S. Babichev, *Izv. Akad. Nauk S.S.S.R., 8* (1976) 1864.
111 V. A. Kuz'min, A. M. Vinogradov, Ya. N. Malkin, M. A. Al'perovich and I. I. Levokev, *Dokl. Akad. Nauk S.S.S.R., 227* (1976) 380.